CHAPTER 3

Chapter 3

Effect of magnetic field on free convection loops

3.1. Introduction

Electrically conducting fluids are abundant in nature, although their conductivities vary greatly. The best conductors of electricity are liquid metals. These are encountered in technology, metallurgy, casting and also in the liquid metal cooling loops of nuclear reactors. In particular, the water in rivers, lakes, sea water and ocean water contain solutions of various salts, so that they conduct electricity. Stronger electrolytes in the form of concentrated solution of acids and alkalis are extensively used in industry. The most prevalent form of electrically conducting fluid in the universe is ionized gas or plasma. All solar and stellar matter is in the plasma state. The upper layers of the earths' atmosphere are also ionized. In addition, interstellar matter consists to a large extent of plasma. Hence, the magnetic fields are a permanent feature of our physical world.

Two distinct virtues make the closed loop thermosyphon profitable to study, although oddly, it has received about the least attention. First, it is a very natural geometric configuration which can be found (or easily created) in many industrial situations. Secondly, it avoids the entry choking or mixing that occurs in the open thermosyphon. Thus, in

addition to being convenient and common, the closed loop thermosyphon should be capable of attaining much larger heat transfer rates.

In principle, there is virtually no limit to the types of flow that could be obtained in a closed loop subject to various thermal, geometric, body force and thermodynamic state conditions. Most cases so far considered have been simple single-phase, continuous loop flows. All analyses to date of the loop flow have been simple one-dimensional force and energy balances.

For the sake of simplification, the loops were studied using the simple configuration of circular toroidal loop heated uniformly over the lower half and cooled over the upper half through a constant wall temperature or annular heat exchanger (Creveling *et al* (1975), Damerell and Schoenhals (1979), Greif *et al* (1979), Mertol *et al* (1981a), Mertol *et al* (1981b), Mertol and Greif (1982), Lavine *et al* (1987)).

Creveling *et al* (1975) treated the toroidal loop without regarding dissipation effects with a constant wall flux inwards for the lower half of the torus and constant wall temperature for the upper half of the torus. They found that steady state solutions of the one-dimensional model equations agreed with experiments only if the wall stress parametrization in terms of the mass flux varied with the applied heating rate.

Zvirin (1979) presented a theoretical evaluation of the effect of dissipation on natural circulation loops heated from below and cooled

from above. He found that for laminar and turbulent flows in the toroidal loop, the steady state velocities are enhanced by dissipation. Wacholder *et al* (1982) presented details of a general numerical method of solution for the toroidal thermosyphon problem.

Yorke and Yorke (1981), Hart (1984) and Malkus (1972) investigated instabilities in a toroidal thermosyphon. They have found that the no-flow solution is unstable when a modified Rayleigh number exceeds a certain critical value. However, they failed to include the conduction term in the energy equation.

The purpose of the present work is to study the effect of dissipation on the free convection loops in the presence of a uniform magnetic field parallel to the plane of the loop. The loss of energy due to Joule heating will be taken into account. An one-dimensional model in which the only space co-ordinate runs around the loop will be used to describe the motion. Stability predictions of this problem will be developed. We will solve numerically the dispersion relation obtained from linear stability analysis of this problem and present the neutral stability curves.

3.2. Mathematical formulation

We consider a vertically oriented, closed toroidal loop shown in figure (3.1) which has a constant circular cross section of radius r. It is considered that the system is subjected to a uniform heat flux over the internal area of its lower half and is cooled by applying a constant wall temperature over the entire internal area of its upper half. A uniform heat flux q is applied at the circumference of the lower half and upper half wall temperature T_w is kept constant. A magnetic field $\vec{B} = (B_r, B_\theta, 0)$ is applied.

The conservation equations are

$$\rho_0 \left[\frac{\partial \vec{v}}{\partial t} + (\vec{v} . \nabla) \vec{v} \right] = - \nabla p + \rho \vec{g} + \vec{F} + \vec{j} \times \vec{B} \qquad (3.2.1)$$

$$\nabla . \vec{v} = 0 \qquad (3.2.2)$$

$$\frac{\partial \vec{H}}{\partial t} = \eta \nabla^2 \vec{H} + \nabla \times (\vec{v} \times \vec{H}) \qquad (3.2.3)$$

$$\nabla . \vec{H} = 0 \qquad (3.2.4)$$

$$\vec{B} = \mu_e \vec{H}$$

where ρ_0 is standard density, ρ the actual density, $\vec{g}$ the acceleration of gravity, μ_e magnetic permeability' and $\vec{F}$ the friction force. The assumption that the Boussinesq approximation is valid is made. Hence the density and temperature have a relation of the form

$$\rho = \rho_0 [1 - \beta (T - T_0)] \qquad (3.2.5)$$

where β is the thermal expansion co-efficient.

The change in magnetic energy which represents a loss of energy resulting from the Joule heating by the currents flowing in the conductor is included in the heat equation. Hence following Chandrasekhar (1981) the heat equation is taken as

$$\rho c \left(\frac{\partial T}{\partial t} + (\vec{v} . \nabla) T \right) = Pq - Ph \left(T - T_w \right) + \frac{1}{A} \int \Phi \, dA + \frac{|\vec{j}|^2}{\sigma_e} \qquad (3.2.6)$$

For the fluid physical model the governing equations applied here are the conservation equations of mass, momentum and energy for a one dimensional, time dependent flow. The only space independent variable is the angular co-ordinate θ.

The analysis of this system has concentrated on the study of one-dimensional models for the flow. That is, cross-sectional averages are taken perpendicular to the circumferential axis of the torus. The non-linear terms in the momentum and energy equations are replaced by interactions between the averaged temperature and the averaged azimuthal mass flux only. This is equivalent to neglecting the averaged Reynolds stress in the usual mean and turbulent flow decomposition. If the averaging is done carefully, one-dimensional models provide a useful and qualitatively accurate description of the observed motion.

Following Welander (1967) and Creveling *et al* (1975), we assume that the tangential friction force on the fluid is proportional to the

instantaneous flow rate Q. Taking $\vec{v}$ = (0, V, 0) equation (3.2.1) results in

$$\rho_0 \frac{dV}{dt} s = \rho_0 g \beta \oint T\, dz - \oint P \tau_w\, ds + \oint \vec{j} \times \vec{B}\, ds \tag{3.2.7}$$

where V is the mean velocity Q/A, (Q = volumetric flow rate); A is the cross sectional area, s is the circulation length, z a vertical co-ordinate and P is the ratio of perimeter to cross sectional area. The wall shear stress τ_w is expressed by $\tau_w = \frac{1}{2} f \rho (V\mu c)^2$ where f is the friction factor and the Reynolds number Re is defined by $\rho_0 2r V / \mu$ where μ is the dynamic viscosity and 2r is the (hydraulic) diameter.

For the purpose of analysis, the correlation between the friction factor and Reynolds number is needed. Toroidal loop correlations were developed using experimental measurements. The rationale employed in constructing these correlations was based on the consideration of steady state conditions only. The values a and b for a friction-factor correlation of the form $f = a/Re^b$ depend on the flow regime (Creveling *et al* (1975)).

Neglecting axial heat conduction, the energy equation is written as

$$\rho c \left(\frac{\partial T}{\partial t} + V \frac{\partial T}{\partial s} \right) = Pq - Ph (T - T_w) + \frac{1}{A} \int \Phi\, dA + \frac{|\vec{j}|^2}{\sigma_e} \tag{3.2.8}$$

where c is the specific heat of the fluid, q denotes heat flux, h is the heat transfer co-efficient, Φ is the dissipation function and the joule dissipation is the last term.

On multiplying equation (3.2.3) by sin θ and integrating around the loop, we get

$$\frac{\partial B_r}{\partial \theta} = - \frac{V B_r r}{\eta} \qquad (3.2.9)$$

from which the equations (3.2.7) and (3.2.8) may be rewritten as (3.2.10) and (3.2.11). At the equilibrium state the magnetic field is taken as (-B cosθ , B sinθ , 0).

According to the assumptions mentioned above, the momentum and energy equations (3.2.7) and (3.2.8) are

$$\frac{\partial^2 V}{\partial t^2} + \frac{\eta}{r^2}\frac{\partial V}{\partial t} + \frac{1}{r} a\, Re^{-b} V \left(2\frac{\partial V}{\partial t} + \frac{\eta}{r^2} V \right) - \frac{B^2 V}{2 \rho r^2 \mu_e}$$

$$= \frac{\beta g}{2\pi} \int_0^{2\pi} \left(\frac{\partial T}{\partial t} + \frac{\eta}{r^2} T \right) \cos\theta \, d\theta \qquad (3.2.10)$$

$$\rho c \left(\frac{\partial T}{\partial t} + \frac{\partial T}{\partial \theta} \right) = - \frac{2h}{r} T + \frac{2}{r^2} \int \Phi r' \, dr' + \frac{V^2 B_r^2}{\sigma_e \eta^2}$$

$$= \frac{2}{r} q + \frac{2}{r^2} \int \Phi r' \, dr' + \frac{V^2 B_r^2}{\sigma_e \eta^2} \qquad \begin{matrix} 0 < \theta < \pi \\ \pi < \theta < 2\pi \end{matrix} \qquad (3.2.11)$$

where T is the temperature above T_w, μ_e permeability and σ_e electrical conductivity.

The friction-factor correlation can be established from experiments thereby making a and b known constants. The correlations are found to be

$$f = 151 / Re^{1.17} \quad \text{for laminar flow}$$

and $$f = 0.88 / Re^{0.45} \quad \text{for turbulent flow}$$

Hence three cases will be considered. The first one being laminar flow with a = 16, b = 1. The other two cases are based on the observations of Creveling *et al* (1975); laminar flow with a = 151, b = 1.17 and turbulent regime with a = 0.88, b = 0.45, transition occurring at Re ~ 1500.

The boundary conditions are given by the continuity of the temperature distribution,

$$T(2\pi) = T(0)$$

and $$T(\pi^{+}) = T(\pi^{-}) \qquad (3.2.12)$$

In cryogenic applications, dissipation is significant and would tend to increase the flow rate in a loop, (Mertol *et al* (1980)). In the present analysis, the dissipation of magnetic energy resulting from the Joule heating by the currents flowing in the conductor is taken into account.

The integration of the pressure terms in equation (3.2.1) adds to zero around the loop. Continuity equation implies that the velocity depends on the temperature.

We non-dimensionalise the above equations (3.2.8) - (3.2.11) by scaling temperature, velocity and time by q/h, U and $2\pi R/U$ respectively. The characteristic velocity U is defined based on the approximate steady state solution obtained by Creveling *et al* (1975), as

$$U = \left(\frac{2^{b+2} r^b \rho_w^{b-1} \beta g q R}{\pi a c \mu^b} \right)^{1/3-b} \qquad (3.2.13)$$

Thus the non-dimensionalised equations are given as

$$\frac{\partial^2 V}{\partial t^2} + \left(\frac{1}{R_m} + \frac{64\pi}{E} V^{1-b} \right) \frac{\partial V}{\partial t} + \frac{32\pi}{E R_m} V^{2-b} - S V$$

$$= \frac{8\pi^2}{DE} \int_0^{2\pi} \left(\frac{\partial T}{\partial t} + \frac{1}{R_m} T \right) \cos\theta \, d\theta \qquad (3.2.14)$$

$$\frac{\partial T}{\partial t} + 2\pi V \frac{\partial T}{\partial \theta} = -2D\,T + (\phi_1 + \phi_2 \cos^2\theta)\, V^2 \qquad 0 < \theta < \pi$$

$$\frac{\partial T}{\partial t} + 2\pi V \frac{\partial T}{\partial \theta} = 2D + (\phi_1 + \phi_2 \cos^2\theta)\, V^2 \qquad \pi < \theta < 2\pi$$

(3.2.15)

where the dependence of the problem on the material properties has been reduced to the following dimensionless parameteres.

$$D = \frac{2\pi R h}{\rho_w c r U}; \quad E = \frac{16 r Re_{Ch}^b}{aR}; \quad Re_{Ch} = \frac{2 r \rho_w U}{\mu}$$

$$\phi_1 = \frac{4 D g\beta R}{\pi c}$$ non-dimensional viscous dissipation

$$\phi_2 = \frac{D E R_m S g\beta R}{4\pi^2 c}$$ non-dimensional joule dissipation

$$R_m = \frac{U r^2}{2\pi R \eta}; \quad \eta = \frac{1}{\mu \sigma_e}; \quad S = \frac{2\pi^2 R^2}{r^2} \frac{\mu B^2}{\rho U^2 \mu_e^2}$$

(3.2.16)

3.3. Analysis of steady state solutions

The stability boundary associated with the onset of motion can be derived from the conditions for existence of a steady flow in the loop. This section deals with the toroidal thermosyphon whose steady state has been extensively investigated by Yorke and Yorke (1981) and Hart (1984). Their analyses were restricted to some severe symmetric conditions on the driving forces of the loop (heating and cooling patterns). Moreover, these analyses exclude the thermal conduction. In the present analysis we have considered the thermal conduction.

The steady state problem is governed by equations (3.2.14) and (3.2.15) without time derivatives and with boundary conditions (3.2.12). If the steady state velocity and temperature are denoted as $\bar{V}$, $\bar{T}$ we have

$$\frac{32\pi}{E R_m}\bar{V}^{2-b} - S\bar{V} = \frac{8\pi^2}{DE R_m}\int_0^{2\pi} \bar{T}\cos\theta \, d\theta \qquad (3.3.1)$$

$$2\pi\bar{V}\frac{\partial \bar{T}}{\partial \theta} = -2D\,\bar{T} + (\phi_1 + \phi_2\cos^2\theta)\,\bar{V}^2 \quad 0 < \theta < \pi$$

$$= 2D + (\phi_1 + \phi_2\cos^2\theta)\,\bar{V}^2 \quad \pi < \theta < 2\pi \qquad (3.3.2)$$

with boundary conditions

$$\bar{T}(2\pi) = \bar{T}(0) \quad \text{and} \quad \bar{T}(\pi^+) = \bar{T}(\pi^-) \qquad (3.3.3)$$

The temperature distributions are obtained by solving the above equation (3.3.2) and then introducing them in the first equation (3.3.1) we can obtain the velocity of steady state. Thus equation (3.3.2) yield the steady state temperature as

$$\bar{T} = C_1 e^{-\frac{D\theta}{\pi \bar{V}}} + \frac{\phi_1 \bar{V}^2}{2D} + \frac{\phi_2 \bar{V}^2}{2D\,(D^2/\pi^2 \bar{V}^2 + 4)} \left[\frac{D^2}{\pi^2 \bar{V}^2} \cos^2\theta + \frac{D}{\pi \bar{V}} \sin 2\theta + 2 \right] \qquad 0 < \theta < \pi$$

$$\bar{T} = \frac{C_2}{2\pi \bar{V}} + \frac{2D + \phi_1 \bar{V}^2}{2\pi \bar{V}}\,\theta + \frac{\phi_2}{4\pi}\left(\theta + \frac{1}{2}\sin 2\theta\right) \bar{V} \qquad \pi < \theta < 2\pi \qquad (3.3.4)$$

Using the boundary conditions (3.3.3), we determine C_1 and C_2 as

$$C_1 = \left(\frac{2D + \phi_1 \bar{V}^2}{2\bar{V}} + \frac{\phi_2 \bar{V}}{4}\right) / \left(1 - e^{-D/\bar{V}}\right)$$

$$C_2 = \frac{\pi \phi_1 \bar{V}^3}{D} + \frac{\pi \phi_2 \bar{V}^3}{D} \frac{(D^2/\pi^2 \bar{V}^2 + 2)}{(D^2/\pi^2 \bar{V}^2 + 4)} - (2\pi D + \phi_1 \pi \bar{V}^2)$$

$$+ \frac{2\pi \bar{V} e^{-D/\bar{V}}}{1 - e^{-D/\bar{V}}} \left(\frac{2D + \phi_1 \bar{V}^2}{2\bar{V}} + \frac{\phi_2 \bar{V}}{4}\right) - \frac{\pi \phi_2 \bar{V}^2}{2} \qquad (3.3.5)$$

This temperature distribution is introduced into equation (3.3.1) leading to the following equation for the steady state velocity,

$$\left(\frac{2D + \phi_1 \bar{V}^2}{2\bar{V}} + \frac{\phi_2 \bar{V}}{4}\right) \frac{D\,(1 + e^{-D/\bar{V}})}{\bar{V}\,(1 - e^{-D/\bar{V}})\,(1 + D^2/\pi^2 \bar{V}^2)} + \frac{2D + \phi_1 \bar{V}^2}{\bar{V}}$$

$$+\frac{\phi_2 \overline{V}}{3}\left(1+\frac{2}{4+D^2/\pi^2\,\overline{V}^2}\right) \;=\; 4\,D\overline{V}^{2-b}-\frac{DE}{8\pi}R_m\,S\,\overline{V} \tag{3.3.6}$$

Equation (3.3.6) is a non-linear algebraic equation for the velocity $\overline{V}$ depending on the parameters D, E, S and R_m. This equation is to be solved numerically and the results are discussed in Section (3.5.).

3.4. Stability characteristics

Single phase thermosyphons may exhibit unstable flows. Here we use the analytical approach to the small amplitude instabilities based on the method suggested by Welander (1967) to discuss the stability of the steady state. The velocity and temperature are written in the following forms:

$$V(t) = \overline{V} + \hat{V}\,e^{\sigma t}; \qquad T(t,\theta) = \overline{T}(\theta) + \hat{T}(\theta)\,e^{\sigma t} \tag{3.4.1}$$

where $\overline{V}$ and $\overline{T}$ denote steady state values, $\hat{V}$ and $\hat{T}$ small perturbations and σ is the stability parameter. The perturbations will grow if the real part of σ (which is generally a complex number) is positive.

In order to calculate the stability parameter σ, V and T from equations (3.4.1) are introduced into the time dependent equations (3.2.7) and (3.2.8). The steady state relations are identically eliminated and then the equations are linearized by neglecting second order terms ($\hat{T}^2$, $\hat{V}^2$, $\hat{T}\,\hat{V}$). Thus the linearized perturbation momentum and energy equations governing the perturbed equations are

$$\sigma^2 \hat{V} + \frac{\sigma}{R_m} \hat{V} + \frac{64\pi}{E} \bar{V}^{1-b} \sigma \hat{V} + \frac{32\pi}{E R_m} (2-b) \bar{V}^{1-b} \hat{V} - S \hat{V}$$

$$= \frac{8\pi^2}{D E} (\sigma + \frac{1}{R_m}) \int_0^{2\pi} \hat{T} \cos\theta \, d\theta \qquad (3.4.2)$$

$$\sigma \hat{T} + 2\pi \bar{V} \frac{\partial \hat{T}}{\partial \theta} + 2\pi \hat{V} \frac{\partial \bar{T}}{\partial \theta}$$

$$= -2D \hat{T} + 2(\phi_1 + \phi_2 \cos^2\theta) \bar{V} \hat{V} \qquad 0 < \theta < \pi$$

$$= 2(\phi_1 + \phi_2 \cos^2\theta) \bar{V} \hat{V} \qquad \pi < \theta < 2\pi \qquad (3.4.3)$$

From equation (3.4.2) it is seen that the velocity depends on the temperature. Therefore, it is necessary to obtain the temperature variations T(θ, t). Thus, from the energy equations for the heated and cooled regions, we obtain,

$$\hat{T} = A \exp[-\frac{\sigma + 2D}{2\pi V} \theta] + \frac{2\bar{V} \hat{V} (\phi_1 + \phi_2 \cos^2\theta)}{\sigma + 2D}$$

$$+ \frac{2D\hat{V}}{\sigma \bar{V} (1 - e^{-D/\bar{V}})} (\frac{2D + \phi_1 \bar{V}^2}{2\bar{V}} + \frac{\phi_2 \bar{V}}{4}) \exp[-\frac{D\theta}{\pi \bar{V}}]$$

$$+ \frac{D \phi_2 \bar{V}^2 \pi \hat{V}}{D^2 + 4\pi^2 \bar{V}^2} \frac{[(\sigma + 2D) \sin 2\theta - 4\pi \bar{V} \cos 2\theta]}{[(\sigma + 2D)^2 + 16\pi^2 \bar{V}^2]}$$

$$- \frac{2\phi_2 \bar{V}^3 \pi^2 \hat{V}}{D^2 + 4\pi^2 \bar{V}^2} \frac{[(\sigma + 2D) \cos 2\theta + 4\pi \bar{V} \sin 2\theta]}{[(\sigma + 2D)^2 + 16\pi^2 \bar{V}^2]} \qquad 0 < \theta < \pi$$

$$\hat{T} = B \exp[-\frac{\sigma\theta}{2\pi \bar{V}}] - \frac{\phi_2 \bar{V} \hat{V}}{2} \frac{[\sigma \cos 2\theta - 4\pi \bar{V} \sin 2\theta]}{[\sigma^2 + 16\pi^2 \bar{V}^2]} - \frac{\phi_2 \bar{V} \hat{V}}{2\sigma}$$

$$+ \frac{2\overline{V}\hat{V}}{\sigma} (\phi_1 + \phi_2 \cos^2\theta) - \frac{\hat{V}}{\sigma\overline{V}} (2D + \phi_1 \overline{V}^2)\, \pi < \theta < 2\pi \tag{3.4.4}$$

where A and B are constants of integration which will be found by applying the following boundary conditions:

$$\hat{T}(0) = \hat{T}(2\pi) \quad ; \qquad \hat{T}(\pi^-) = \hat{T}(\pi^+)$$

Hence the integration constants are obtained as

$$A = C_1 \hat{V}$$

$$B = C_2 \hat{V}$$

$$C_1 = C_2 e^{-\sigma/\overline{V}} + \frac{4D\overline{V}(\phi_1 + \phi_2)}{\sigma(\sigma + 2D)} - \frac{2D + \phi_1\overline{V}^2}{\sigma\overline{V}} - \frac{\phi_2 \overline{V}\sigma}{2(\sigma^2 + 16\pi^2\overline{V}^2)}$$

$$- \frac{\phi_2\overline{V}}{2\sigma} - \frac{2D}{\sigma\overline{V}(1 - e^{-D/\overline{V}})} \left(\frac{2D + \phi_1\overline{V}^2}{2\overline{V}} + \frac{\phi_2\overline{V}}{4}\right)$$

$$+ \frac{2\phi_2\overline{V}^3(\sigma + 4D)\pi^2}{(D^2 + 4\pi^2\overline{V}^2)\,[(\sigma + 2D)^2 + 16\pi^2\overline{V}^2]}$$

$$C_2 = \left\{ \frac{2\phi_2\overline{V}^3(\sigma + 4D)\pi^2}{(D^2 + 4\pi^2\overline{V}^2)\,[(\sigma + 2D)^2 + 16\pi^2\overline{V}^2]} + \frac{4D\overline{V}(\phi_1 + \phi_2)}{\sigma(\sigma + 2D)} \right.$$

$$\left. - \frac{2D + \phi_1\overline{V}^2}{\sigma\overline{V}} - \frac{\phi_2\overline{V}}{2\sigma} - \frac{\phi_2\overline{V}\sigma}{2(\sigma^2 + 16\pi^2\overline{V}^2)} \right\} \frac{(1 - e^{(\sigma + 2D)/2\overline{V}})}{(e^{D/\overline{V}} - e^{-\sigma/\overline{V}})}$$

$$+ \frac{2D}{\sigma\overline{V}(e^{D/\overline{V}} - e^{-\sigma/\overline{V}})} \left(\frac{2D + \phi_1\overline{V}^2}{2\overline{V}} + \frac{\phi_2\overline{V}}{4}\right) \frac{e^{\sigma/2\overline{V}} - 1}{1 - e^{-D/\overline{V}}} \tag{3.4.5}$$

Substitution of the perturbed temperature $\hat{T}(\theta, t)$ from equations (3.4.4) into the momentum equation (3.4.2) yields the following relation for stability parameter σ.

$$
\begin{aligned}
Y(\sigma) \;=\; & \frac{2\pi\overline{V}\, C_1\,(\sigma+2D)\,(1+e^{-(\sigma+2D)/2\overline{V}})}{[(\sigma+2D)^2+4\pi^2\overline{V}^2]} - \frac{8\pi\,\phi_2\,\overline{V}^2}{3\,(\sigma^2+16\pi^2\overline{V}^2)} \\
& + \frac{4\pi\phi_2\overline{V}^2\,[D(\sigma+2D)-8\pi^2\overline{V}^2]}{3\,(D^2+4\pi^2\overline{V}^2)\,[(\sigma+2D)^2+16\pi^2\overline{V}^2]} - \frac{DE\sigma}{8\pi^2} \\
& + \frac{2\pi D^2\,(1+e^{-D/\overline{V}})}{\sigma\,(D^2+\pi^2\overline{V}^2)\,(1-e^{-D/\overline{V}})}\left(\frac{2D+\phi_1\overline{V}^2}{2\overline{V}}+\frac{\phi_2\,\overline{V}}{4}\right) \\
& - \frac{2\pi\,\overline{V}\,\sigma\,C_2\,e^{-\sigma/2\overline{V}}}{(\sigma^2+4\pi^2\overline{V}^2)}\,(1+e^{-\sigma/2\overline{V}}) \\
& - \frac{4D\,\overline{V}^{1-b}\,R_m}{\pi\,(\sigma R_m+1)}\left(2\sigma+\frac{2-b}{R_m}\right) + \frac{D\,E\,S\,R_m}{8\pi^2\,(\sigma R_m+1)} \qquad (3.4.6)
\end{aligned}
$$

Marginal stability curves (vanishing of the real part of σ) in the E - D plane are obtained from equations (3.4.6) in a method similar to that of Creveling *et al* (1975) and Zvirin (1979). The results are presented in the following section.

3.5. Numerical results

The steady state motion and instability characteristics of the circular loops caused by heating uniformly the lower half and cooling by constant

wall temperature at the upper half have been studied by several authors. But most of the existing models for natural circulation loops do not take into account viscous heating of the fluid. Zvirin (1979) was the first to study the effect of dissipation on free convection loops.

We have aimed at studying the effect of dissipation on the toroidal loop in the presence of a uniform two-dimensional magnetic field applied normal to the plane of the loop. In the previous section we have derived some analytical results from which the steady state velocity and the stability characteristics of a toroidal loop may be discussed, taking into account the loss of energy due to Joule heating.

A numerical solution of equation (3.3.6) yields the results shown in figures (3.2) - (3.15) for the steady state velocity $\overline{V}$ as a function of D for various values of the ratio ϕ_1 / D, ϕ_2 / D and SR_mE. From equation (3.3.6), it can be seen that effect of the parameters S, R_m, E on the steady state velocity are given by the last term of equation (3.3.6). Thus when either one of the parameters vanishes, the steady state velocity is unaffected by the remaining parameters. Hence, it is sufficient to study the effect of any one of the three parameters on $\overline{V}$ from which the same result may be deduced for the other two parameters.

In figures (3.2) - (3.7) we have given the variation of the steady state velocity $\overline{V}$ with respect to D for various values of ϕ_2 / D (= 0.0, 0.1, 0.5) keeping ϕ_1 / D =0.0 and S = 0.0 and 5.0. We can conclude

from these figures that steady state flow rate increases with increasing ϕ_2/D.

In figures (3.8) - (3.13), the dependence of the steady state velocity on D for various values of the ratio ϕ_1 / D keeping ϕ_2 / D and S fixed. The ratio ϕ_1 / D for laminar flows with a parabolic velocity profile would be very small (less than 10^{-3}) in a loop of the type investigated by Creveling *et al* (1975). However, the value of this dissipation parameter will considerably increase for turbulent flows: moreover, according to the observations of Damerell and Schoenhals (1978), the velocity profile is much more complicated, including regions of reversed flow. This would be associated with more viscous dissipation. Finally, since the parameter ϕ_1 depends linearly on the thermal expansion co-efficient β, the effect of dissipation will be most important in cryogenic applications, where β has relatively large values.

As can be seen from figures (3.8) - (3.13) dissipation tends to increase the steady state flow rate. This may be explained as follows: the heat input of the source is a given constant; the effect of dissipation is a further temperature increase of the fluid. At steady state this energy has to be transfered out by the circulating fluid. Hence the flow rate in the loop increases.

In figures (3.14) and (3.15), the effect of magnetic field on the steady state velocity is given. It can be deduced that the increase in the magnetic field increases the steady state velocity.

From figures (3.2) - (3.15), it is seen that for large values of D, a change in D effects a minor change in the steady state velocity. D, defined as $2\pi Rh / \rho wcrU$, is large implies that the heat transfer co-efficient h is large which causes smaller temperature and therefore smaller buoyancy. Hence the velocity is small.

Curves of marginal stability (vanishing of the real part of σ) in the E-D plane are obtained from equation (3.4.6) in a method similar to that of Creveling *et al* (1975) and Zvirin (1979). Since the stability of the system is determined by the values of D and E, the regions of stability and instability can be illustrated by plotting the boundary between the regions (locus of neutral stability) in D,E co-ordinates. The neutral stability condition corresponds to the situation where the $Y(i\omega)$ contour passes through the origin of the $Y(\sigma)$ plane. Thus, points on the stability boundary in the E-D plane are determined by searching for pairs of D and E values for which $Y = Y_r + iY_i = 0$. This occurs when both Y_r and Y_i are zero at some frequency ω, which is unknown at the start of the search procedure. This approach was initially developed by Welander (1967) in the determination of neutral stability conditions and was later

used by Creveling *et al* (1975) for the prediction of stability characteristics.

We proceed initially to choose a value of D. For this value of D, we find the steady state velocity $\overline{V}$, E and the imaginary part of the frequency ω so as to satisfy equations (3.3.6) and (3.4.6) from which the marginal stability curves in the E-D plane are drawn. These curves are presented in figures (3.16) - (3.22). As mentioned earlier, the curves depicted in figures (3.16) - (3.22) correspond to three cases: laminar flow with a =16, b =1, laminar flow with a =151, b =1.17 and turbulent flow with a =0.88, b =0.45.

In figure (3.16) we have displayed the marginal stability curves for R_m=S =0. We obtain similar curves when either S or R_m vanishes (Figures (3.17) - (3.20)).

When both R_m and S non-zero, the results obtained for laminar flow (b =1.0, 1.17) are shown in figures (3.21) and (3.22). It can be seen that the increase in the magnetic parameter enlarges the region of stability.

3.6. Conclusion

A theoretical method is presented for the evaluation of the effect of dissipation on natural circulation loops (thermosyphons) created by heating from below and cooling from above. The method is applied to a

toroidal loop that is oriented in a vertical plane and is heated by a uniform heat flux at the lower half and cooled by a constant wall temperature at the upper half. The system is represented by an one-dimensional model, with the only space co-ordinate running along the loop. The fluid taken here is an electrically conducting one and a constant magnetic field perpendicular to the plane of the loop is applied.

Integral forms of the momentum and energy equations are derived and solved to yield the velocity and temperature distributions. The steady state solution is obtained and the linear stability analysis of the system is carried out by perturbing the steady state.

For laminar and turbulent flows, the steady state velocities are enhanced by dissipation. Curves of marginal stability for various dissipation factors are drawn and interpreted.

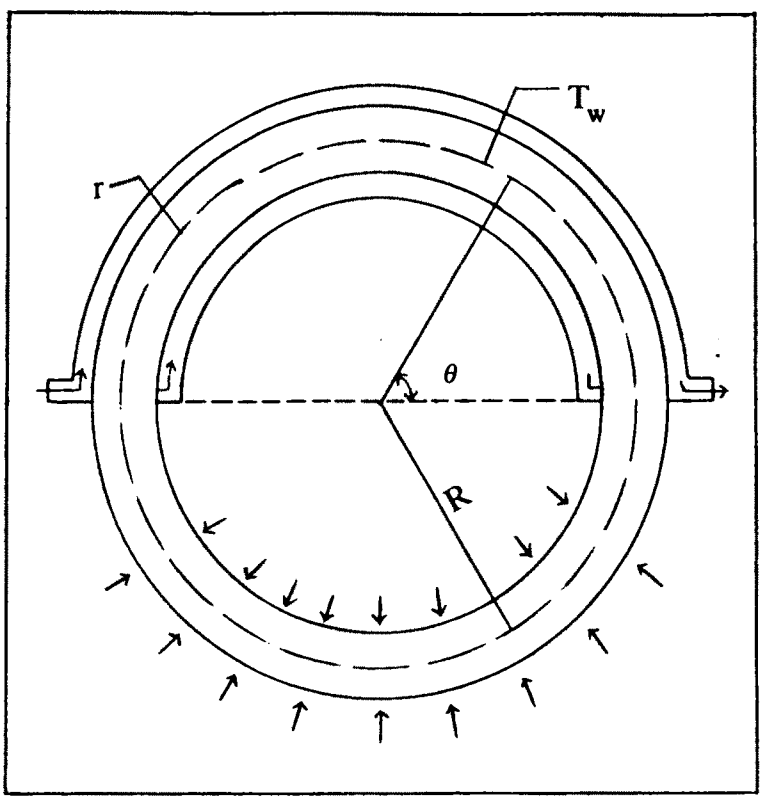

Fig. 3.1. A general representation of toroidal thermosyphon

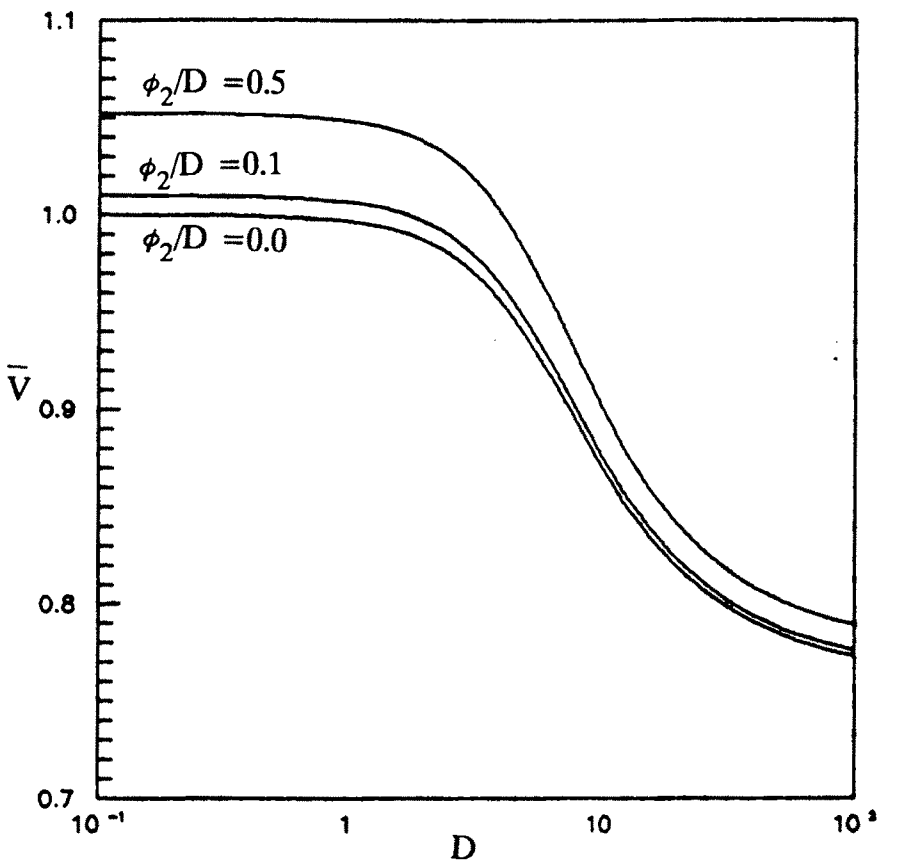

Fig. 3.2. Steady state velocity $\bar{V}$ as a function of D and for various values of ϕ_2 / D
(S = 0.0, b = 0.45)

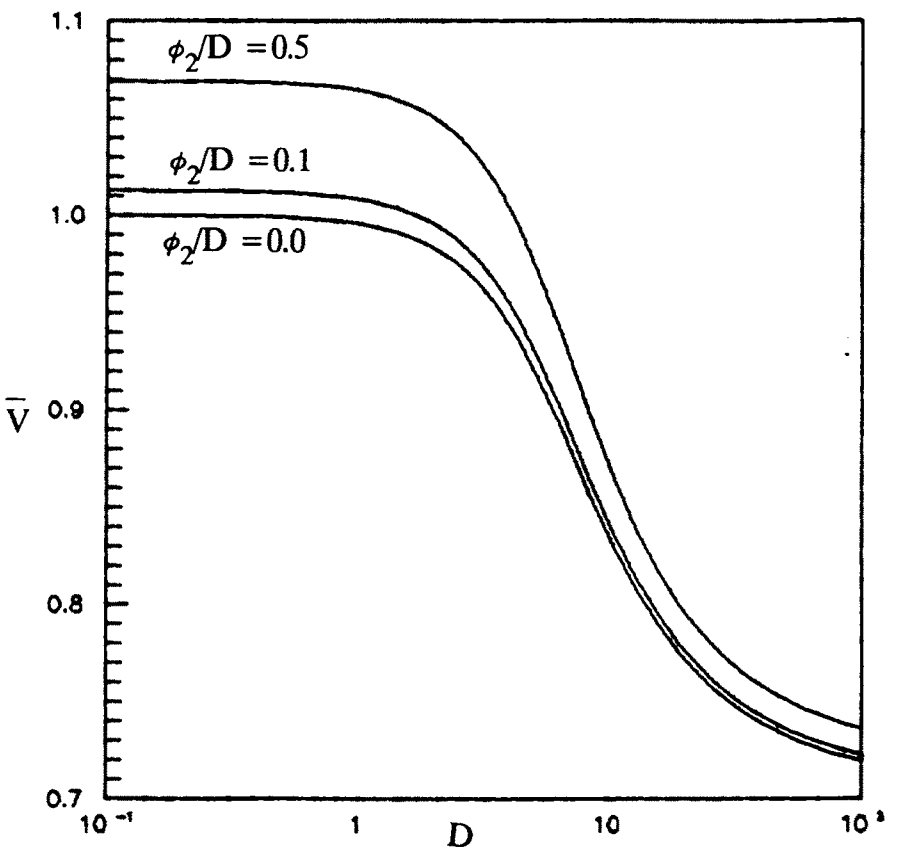

Fig. 3.3. Steady state velocity $\bar{V}$ as a function of D and for various values of ϕ_2 / D
(S = 0.0, **b** = 1.00)

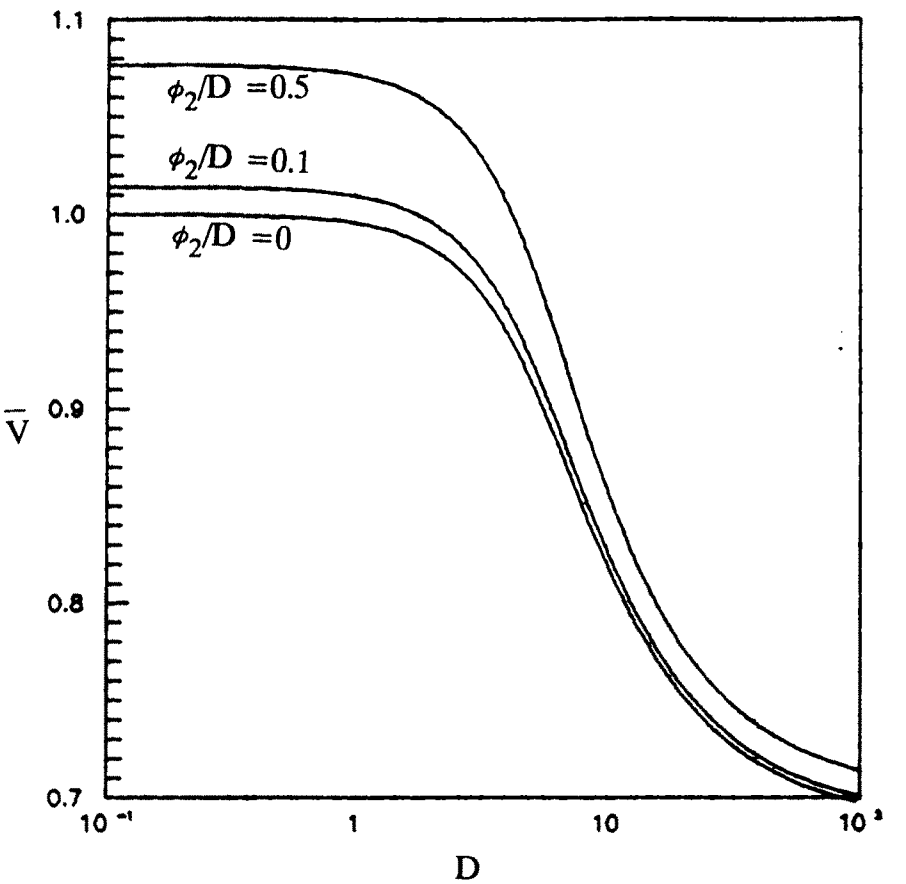

Fig. 3.4. Steady state velocity $\bar{V}$ as a function of D and for various values of ϕ_2 / D
(S = 0.0, b = 1.17)

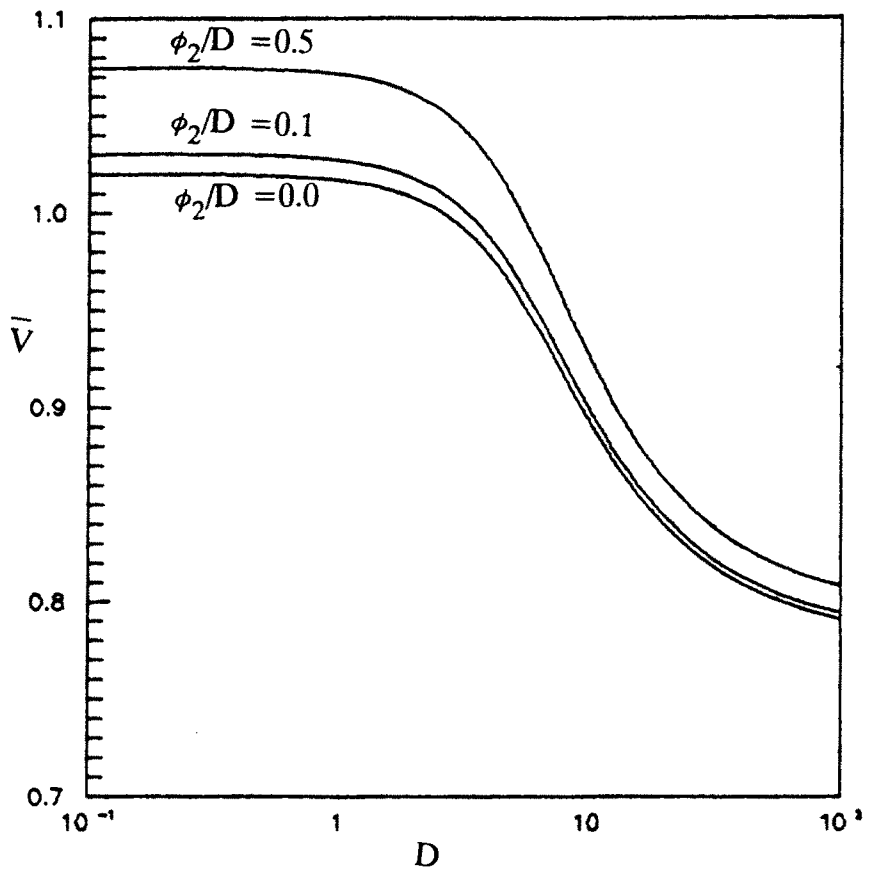

Fig. 3.5. Variation of steady state velocity $\bar{V}$ with respect to D for different values of ϕ_2 / D (b = 0.45, S = 5.0)

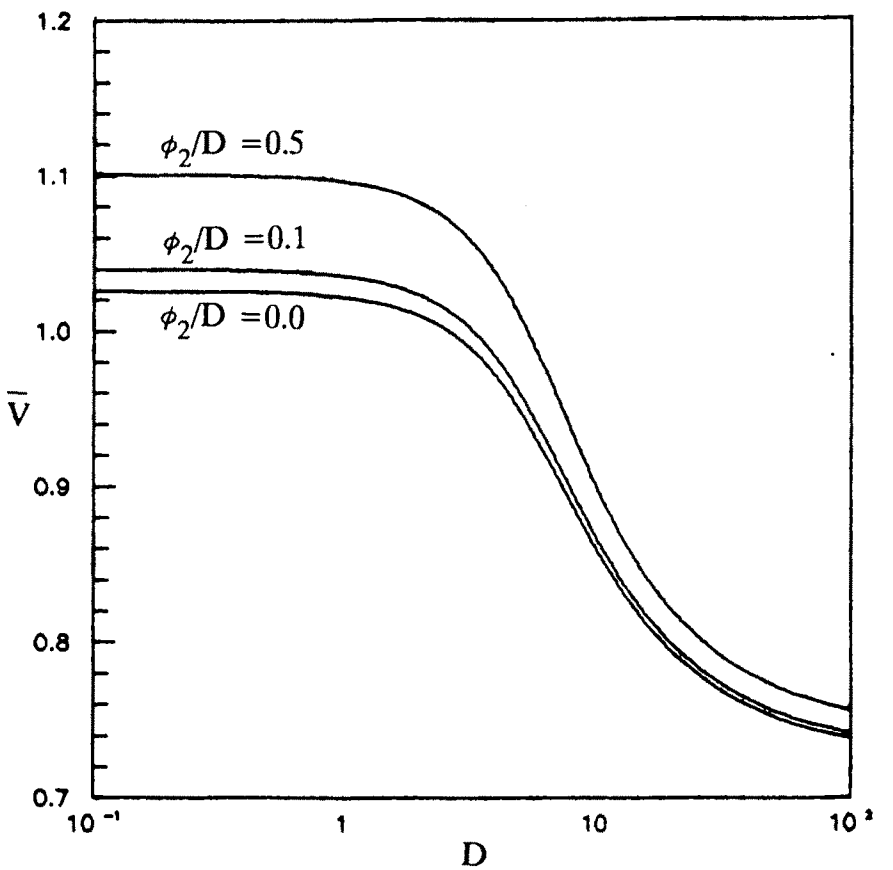

Fig. 3.6. Variation of steady state velocity $\bar{V}$ with respect to D for different values of ϕ_2 / D (b = 1.00, S = 5.0)

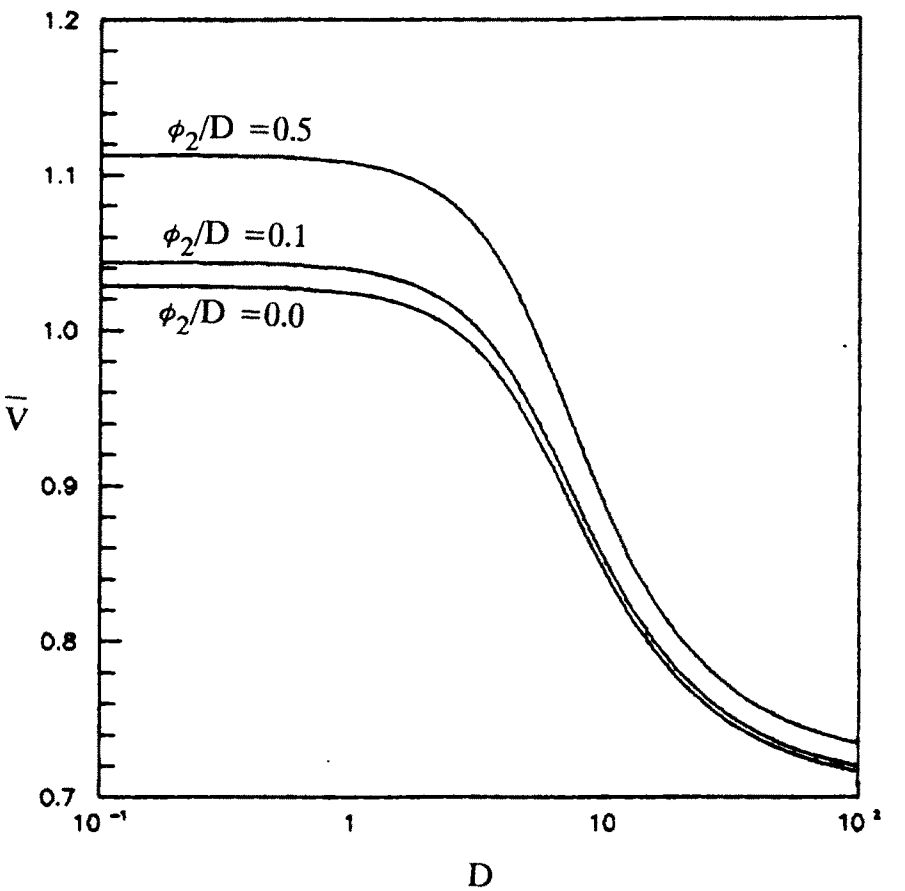

Fig. 3.7. Variation of steady state velocity $\bar{V}$ with respect to D for different values of ϕ_2 / D (b = 1.17, S = 5.0)

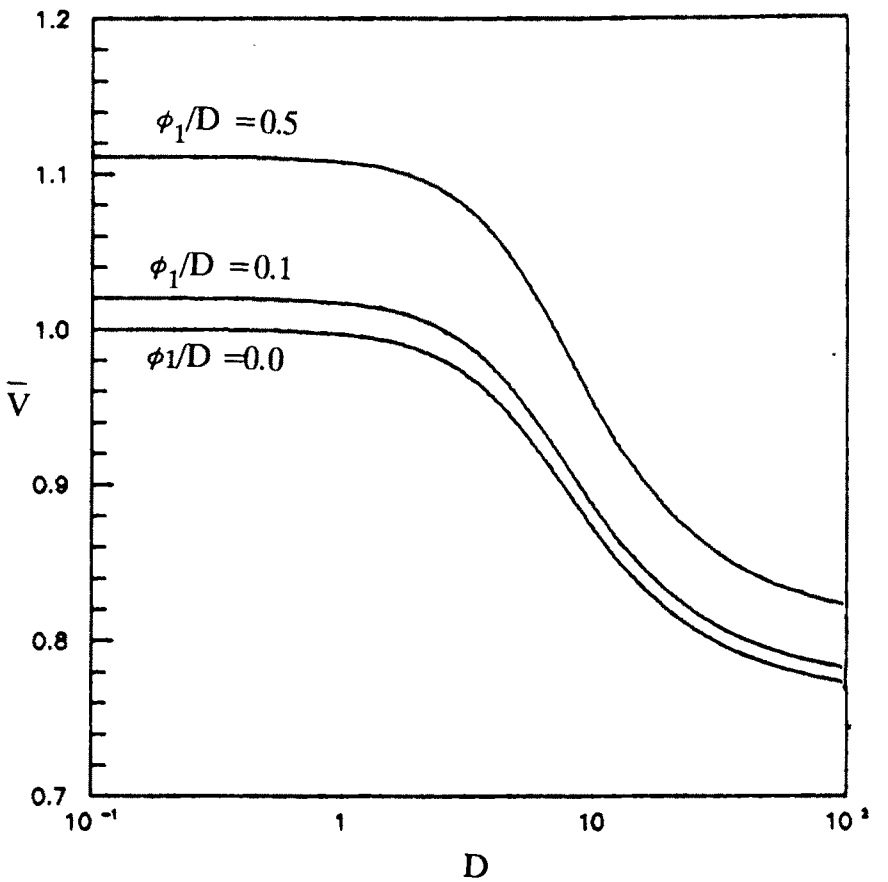

Fig. 3.8. Dependence of $\bar{V}$ on D and ϕ_1/D
(b = 0.45, S = 0.0)

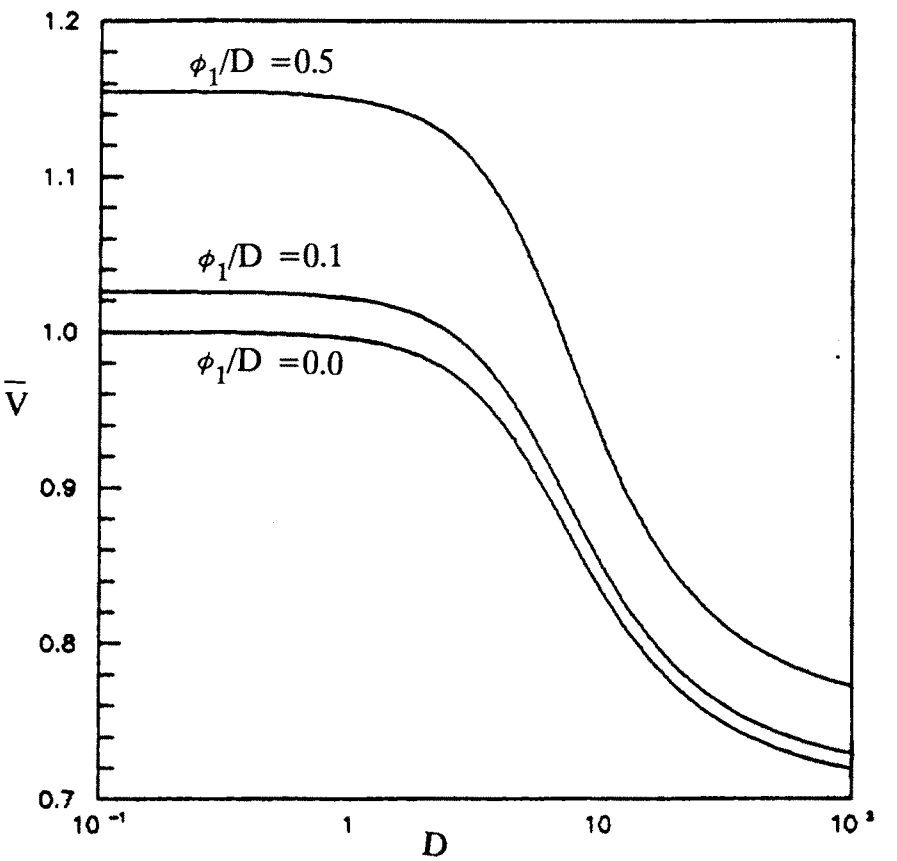

Fig. 3.9. Dependence of $\bar{V}$ on D and ϕ_1 / D
(b = 1.00, S = 0.0)

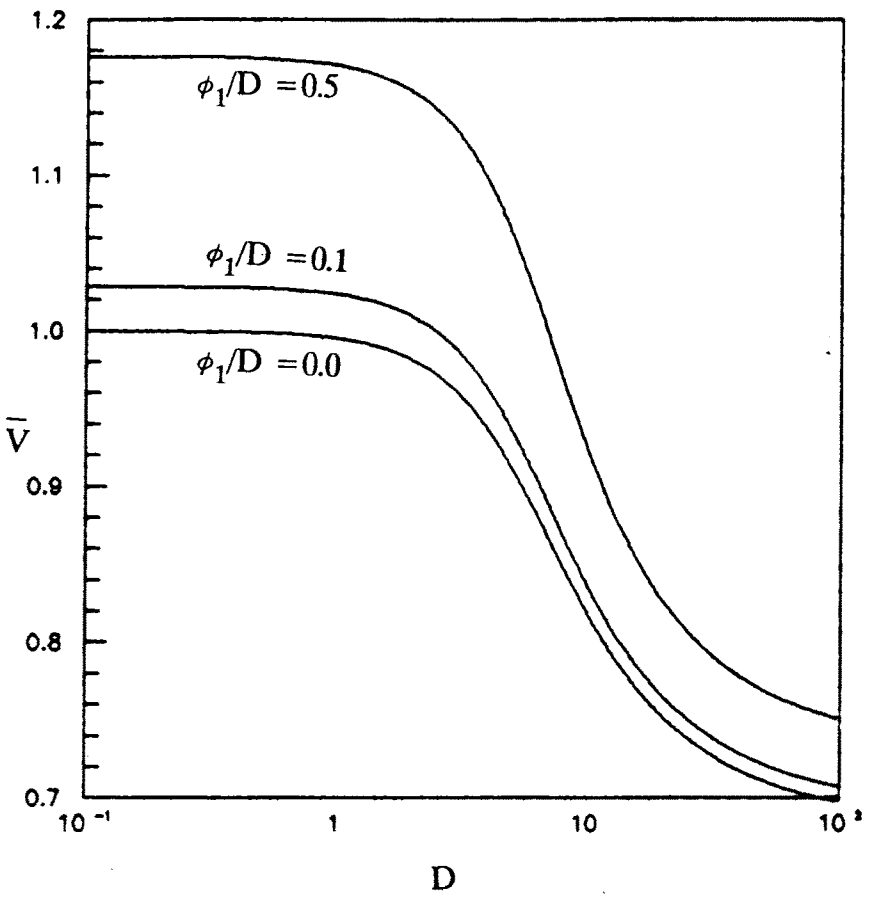

Fig. 3.10. Dependence of $\bar{V}$ on D and ϕ_1 / D
(b = 1.17, S = 0.0)

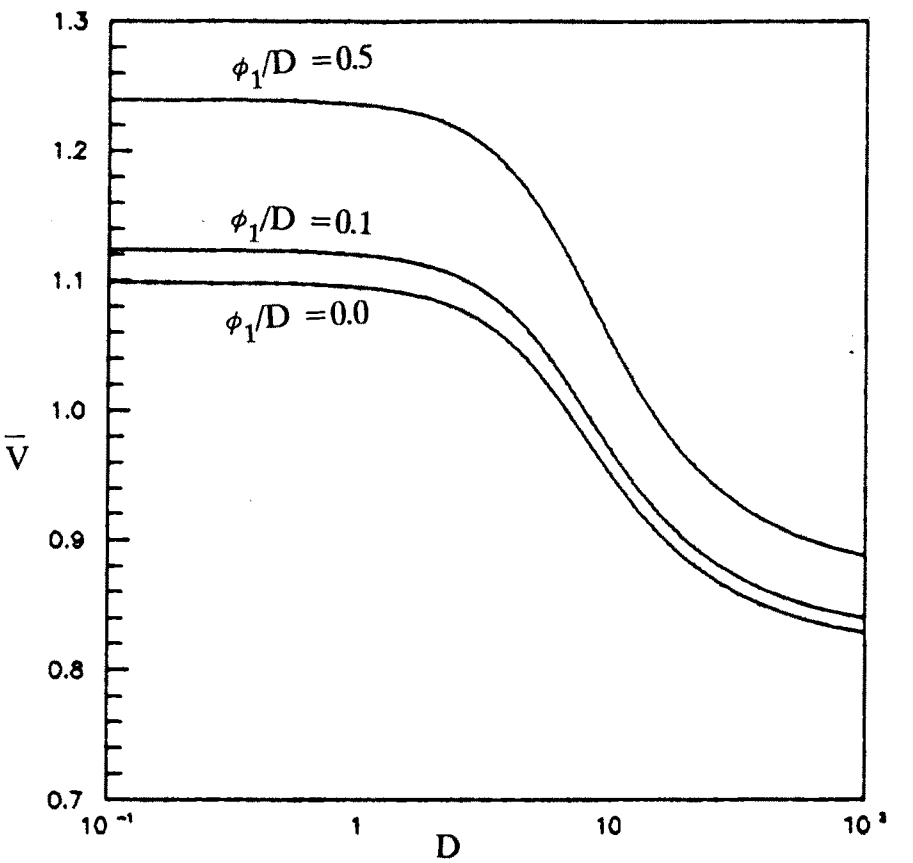

Fig. 3.11. Steady state velocity $\bar{V}$ as a function of D and for various values of ϕ_1/D
(S = 10.0, b = 0.45)

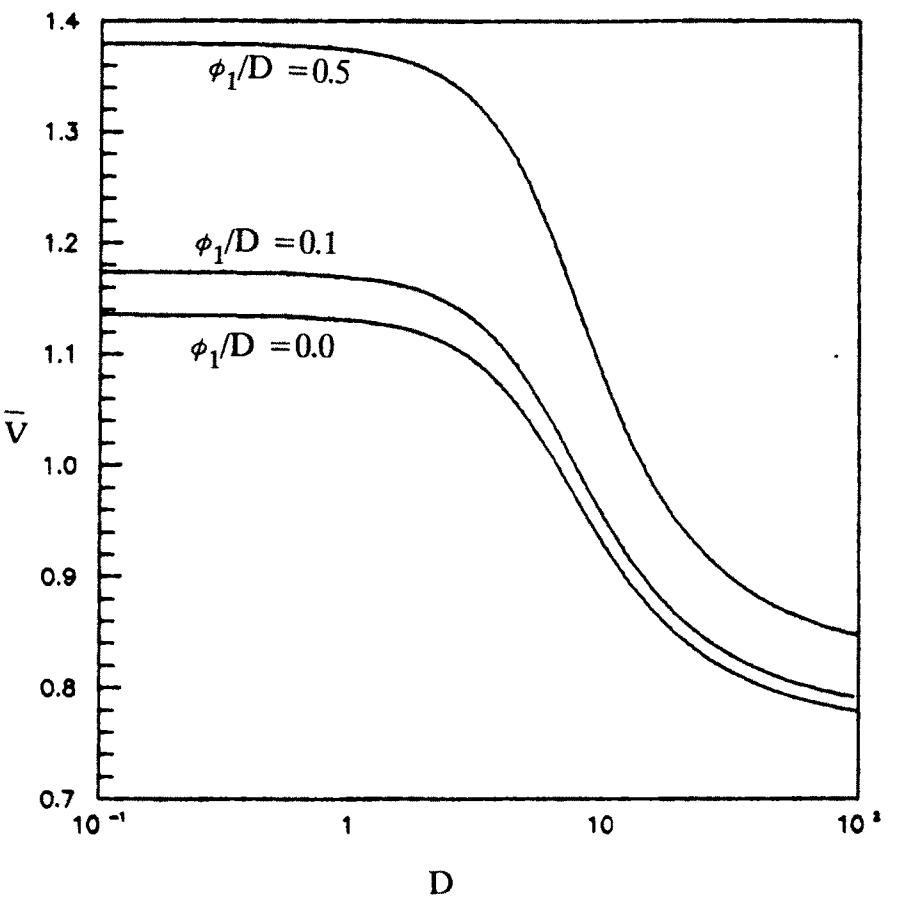

Fig. 3.12. Steady state velocity $\bar{V}$ as a function of D and for various values of ϕ_1/D
(S = 10.0, b = 1.00)

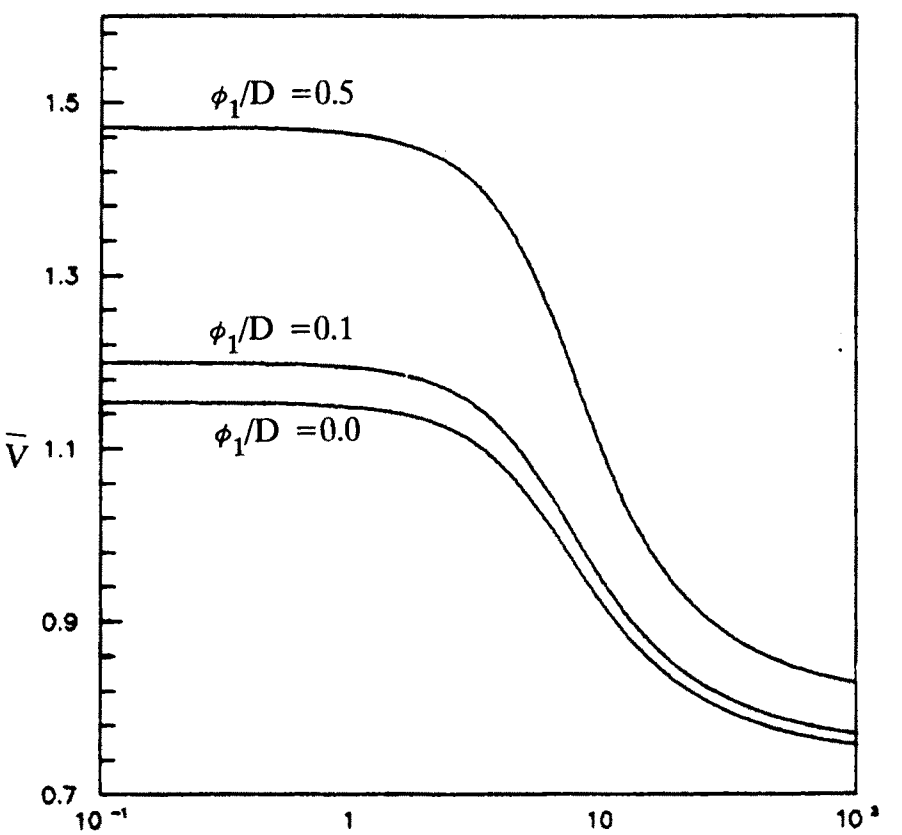

Fig. 3.13. Steady state velocity $\bar{V}$ as a function of D and for various values of ϕ_1 / D
(S = 10.0, b = 1.17)

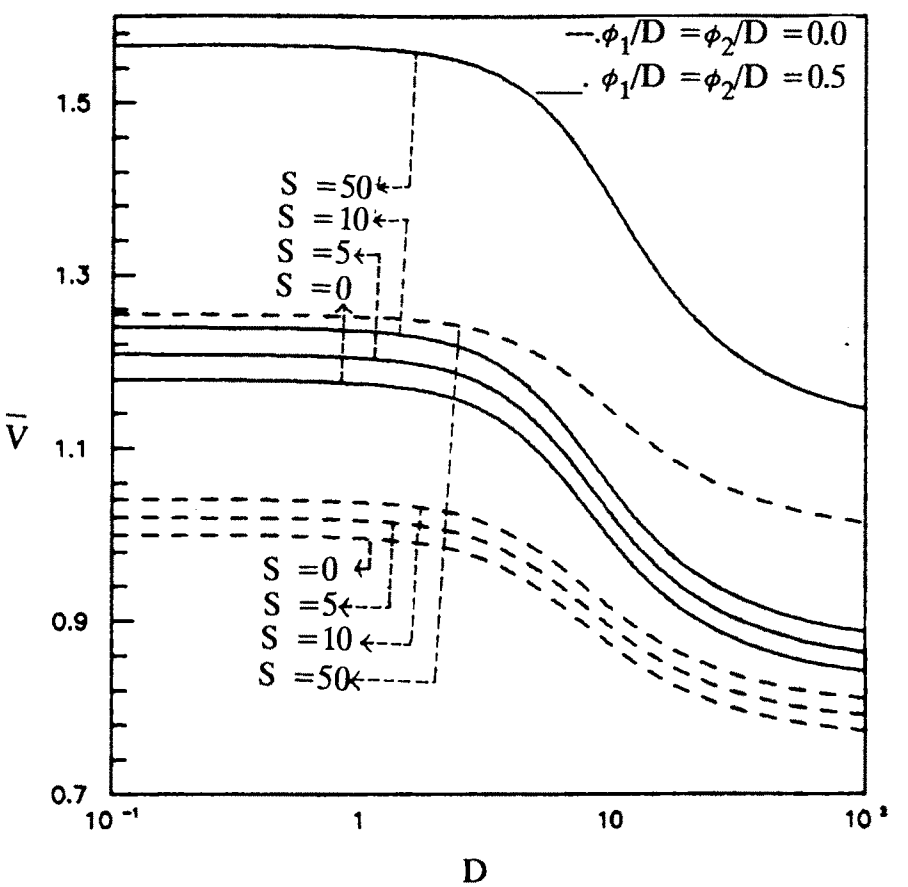

Fig. 3.14. Steady state velocity $\bar{V}$ versus D (b = 0.45)

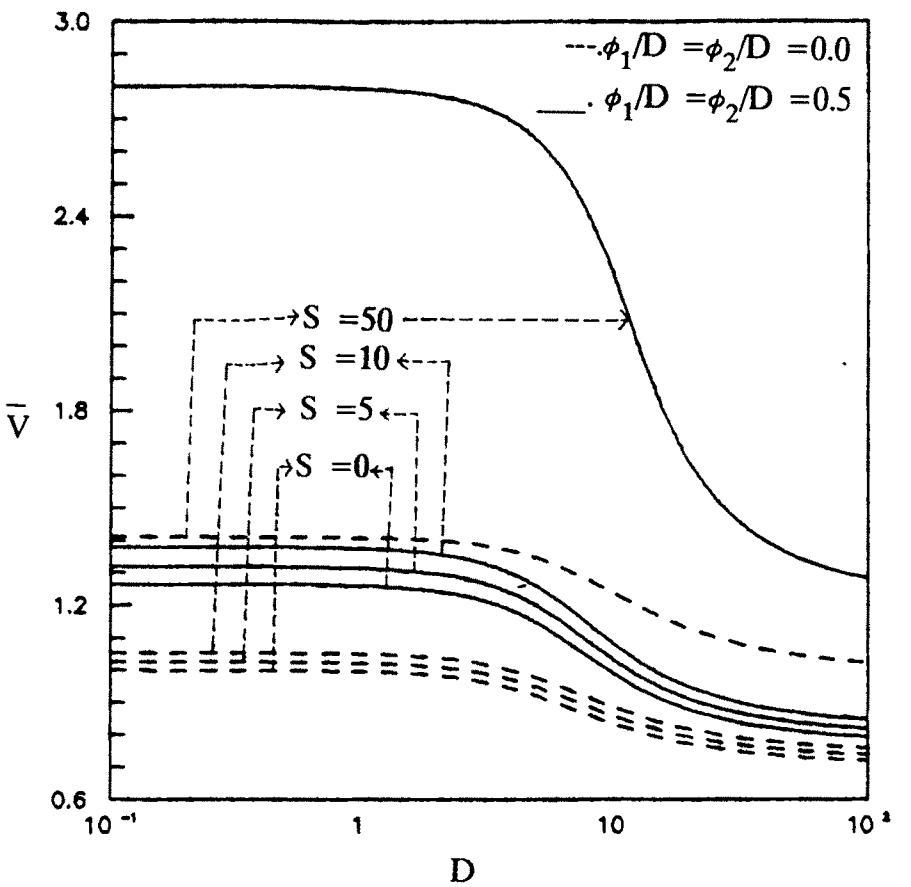

Fig. 3.15. Steady state velocity $\bar{V}$ versus D (b = 1.00)

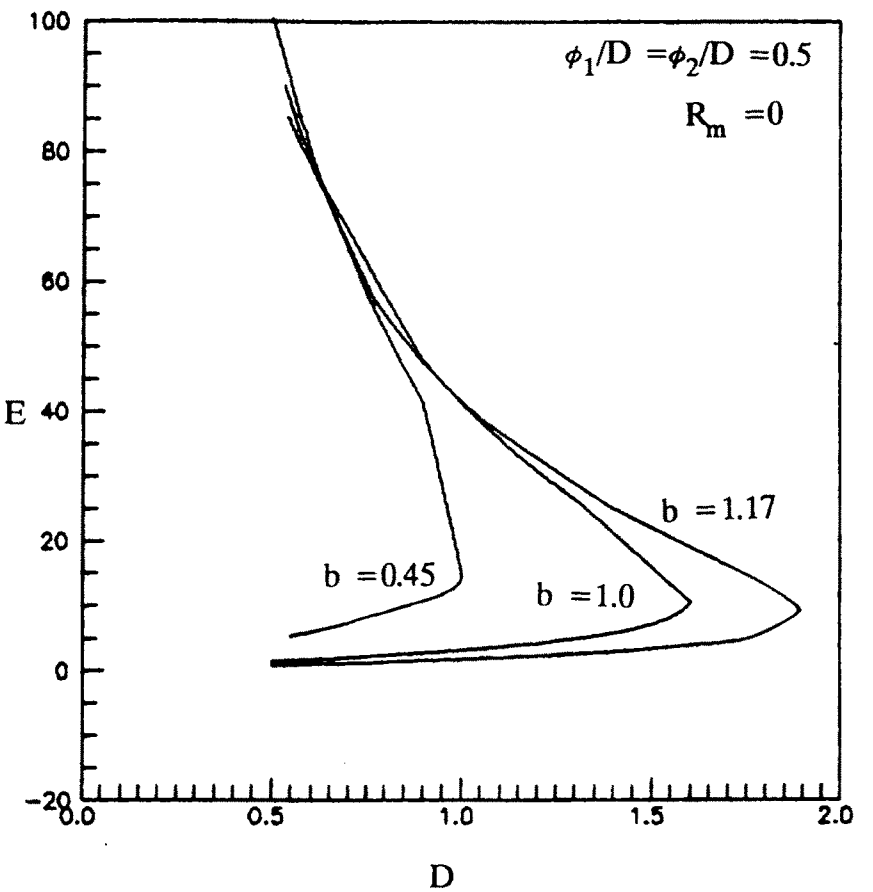

Fig. 3.16. Marginal stability curves in (E, D) plane (S = 0.0)

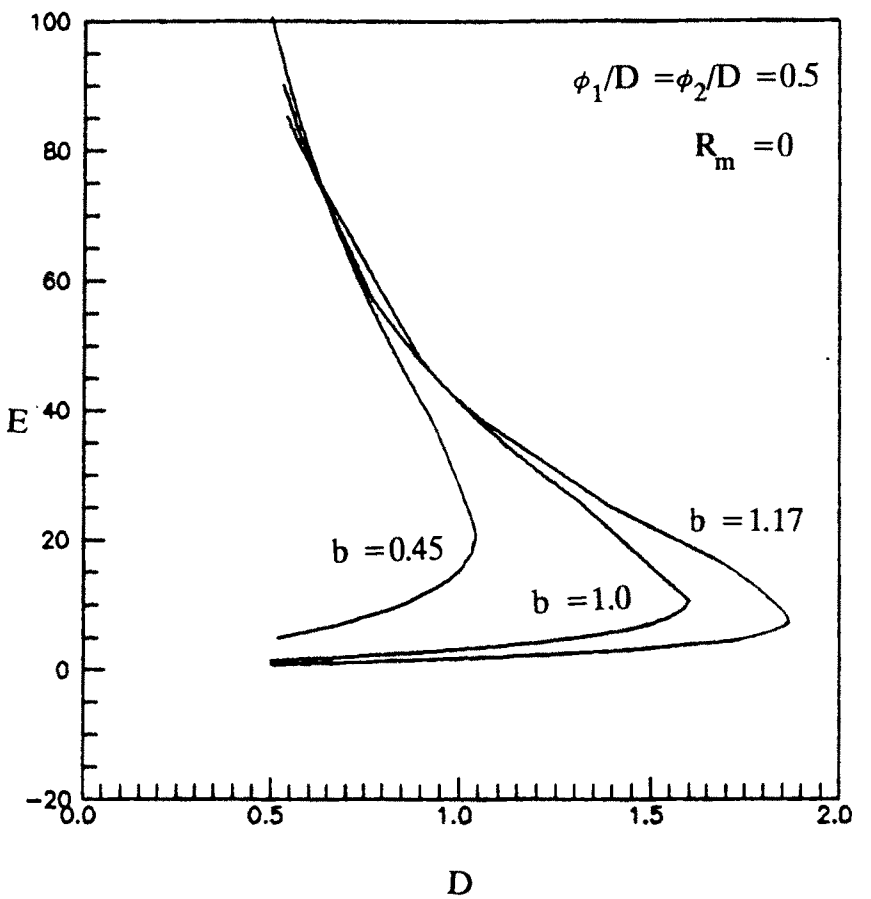

Fig. 3.17. Marginal stability curves in (E, D) plane (S = 5.0)

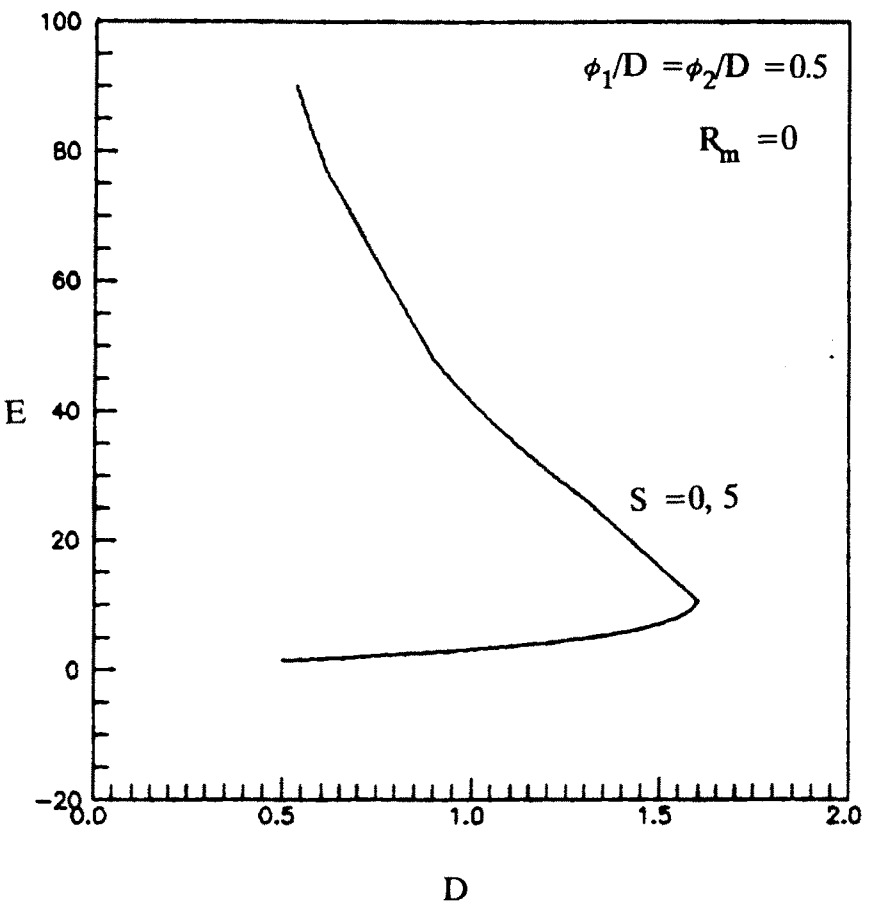

Fig. 3.18. Effect of magnetic field on the marginal stability curves for b = 1.0

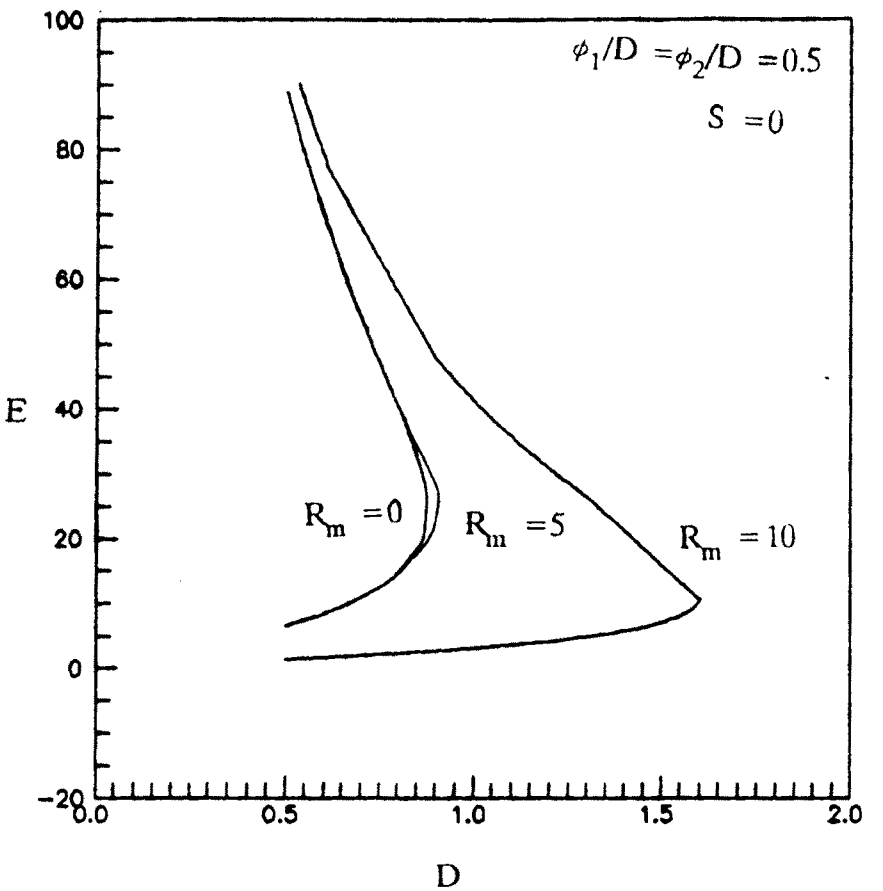

Fig. 3.19. Effect of R_m on the marginal curves (b = 1.0)

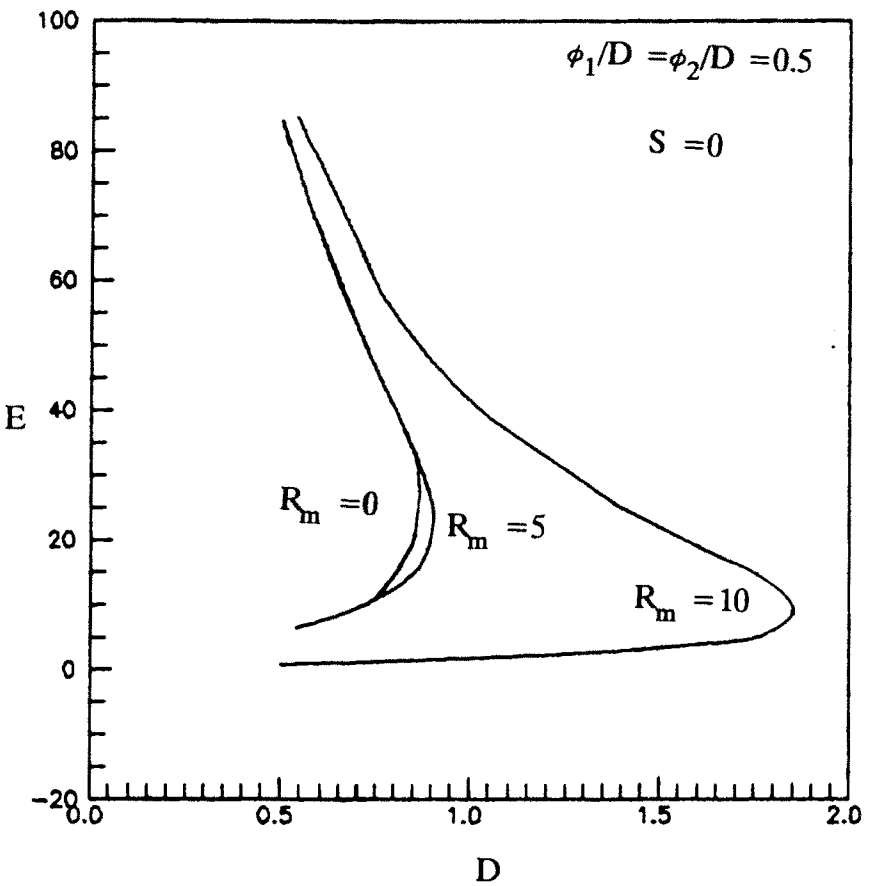

Fig. 3.20. Effect of R_m on the marginal stability curves (b = 1.17)

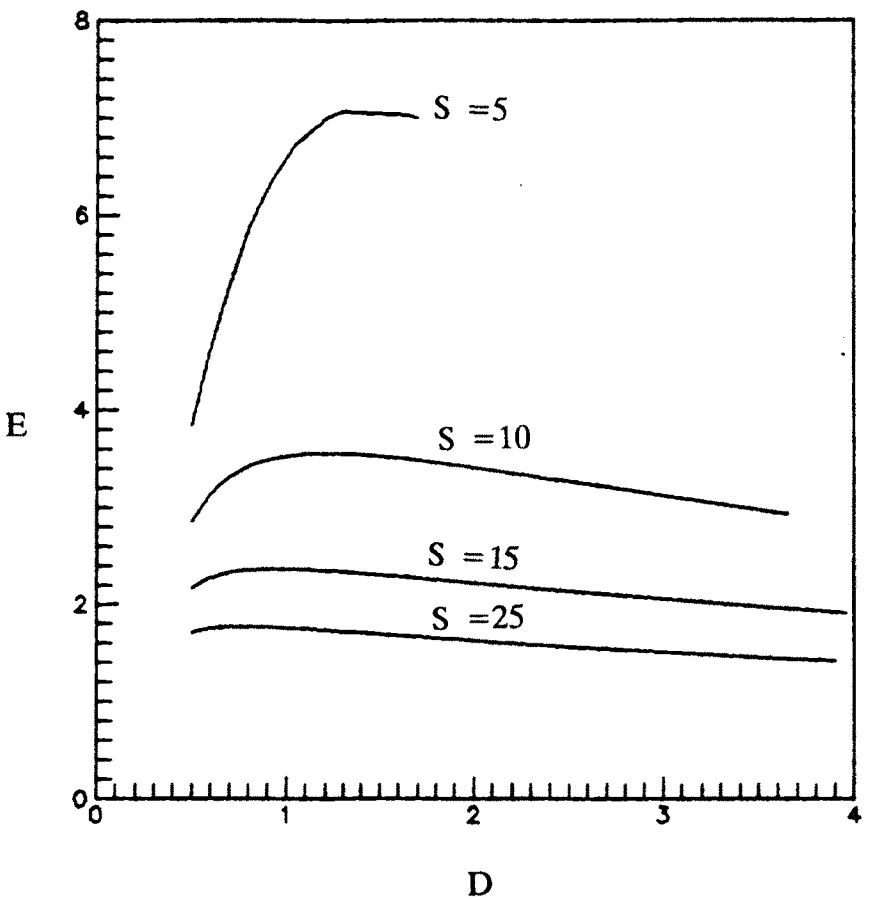

Fig. 3.21. Influence of magnetic interaction number S on the marginal stability of the toroidal thermosyphon (b = 1.0)

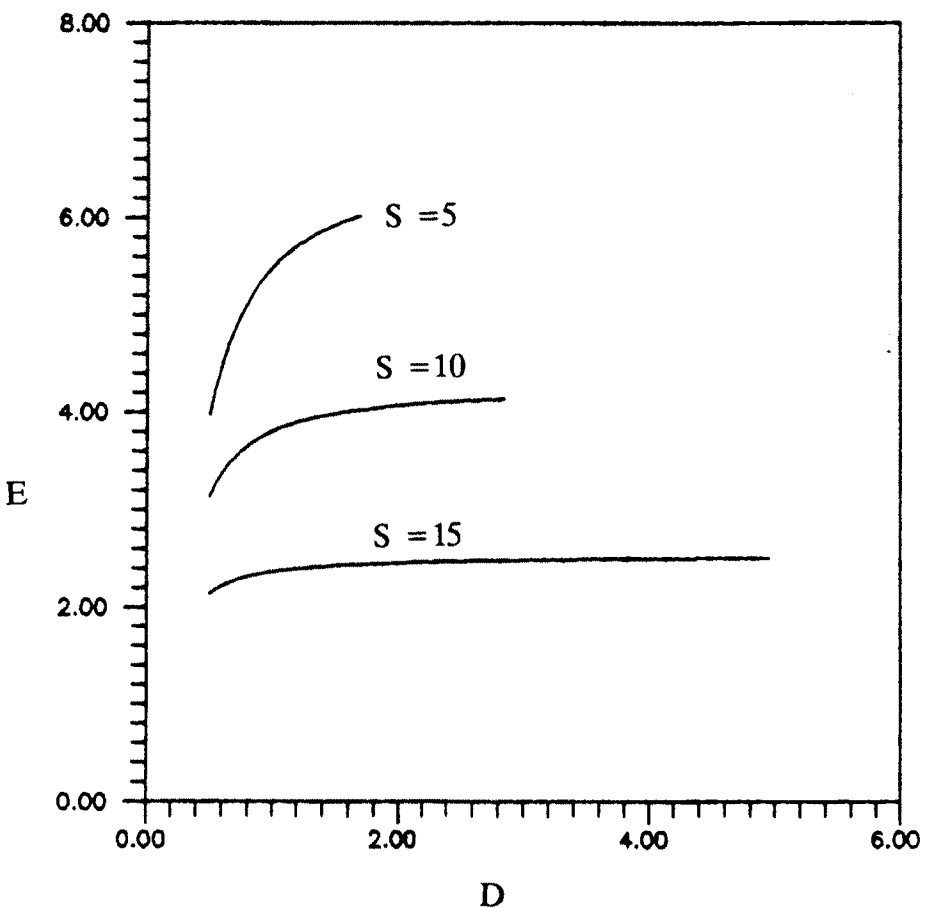

Fig. 3.22. Influence of magnetic interaction number S on the marginal stability of the toroidal thermosyphon (b = 1.17)